IEEE Access
Multidisciplinary | Rapid Review | Open Access Journal

Received April 25, 2019, accepted May 8, 2019, date of publication May 14, 2019, date of current version May 28, 2019.

Digital Object Identifier 10.1109/ACCESS.2019.2916554

Influence of Rotor-Bearing Coupling Vibration on Dynamic Behavior of Electric Vehicle Driven by In-Wheel Motor

YUEWEI YU, LEILEI ZHAO, AND CHANGCHENG ZHOU
School of Transportation and Vehicle Engineering, Shandong University of Technology, Zibo 255049, China

Corresponding author: Changcheng Zhou (greatwall@sdut.edu.cn)

This work was supported in part by the National Natural Science Foundation of China, under Grant 51575325.

ABSTRACT In order to analyze the influence of the rotor-bearing coupling vibration on the dynamic performance of electric vehicles driven by an in-wheel motor, taking a typical four-phase 8/6-pole switched reluctance motor driven electric vehicle without deceleration mechanism as an investigated object, a nonlinear dynamic model of an electric vehicle with the in-wheel motor driving system is established on the basis of considering the motor exciting force and the bearing nonlinear force. Through the numerical simulation, the influence of the rotor-bearing coupling vibration on the dynamic behavior of electric vehicle driven by the in-wheel motor is studied. Here, in this paper, the dynamic characteristics of an electric vehicle with and without motor exciting force and bearing nonlinear force are compared and analyzed. In addition, the influence of the suspension parameters on the dynamic performance of electric vehicle driven by the in-wheel motor is analyzed. According to the results, the influence of the rotor-bearing coupling vibration on the dynamic behavior of the electric vehicle is mainly embodied in the tire vibration acceleration and tire dynamic load. Moreover, the existence of the in-wheel motor driving system will deteriorate the evaluation index of the electric vehicle vibration performance. By choosing appropriate parameters of the vehicle suspension system, the ride comfort of the electric vehicle can be effectively improved.

INDEX TERMS Electric vehicle, driven by in-wheel motor, rotor-bearing coupling vibration, motor exciting force, bearing nonlinear force, dynamic analysis.

I. INTRODUCTION

Due to the aggravation of environmental pollution and energy crisis, electric vehicles have become an important research direction of reducing emissions and saving energy technology. Among many electric vehicles with different driving modes, the electric vehicle driven by in-wheel motor has attracted wide attention because of their simple space layout, small installation space, low energy consumption and low environmental pollution [1]–[3].

In previous studies on the vibration characteristics of electric vehicles driven by in-wheel motor, the influence of the transmission components (such as the motor and the bearing) on the vehicles dynamic is usually neglected, and only the dynamic performance of vehicles under road exciting is studied [4]–[6]. In theory, this method is feasible when the geometric center of the in-wheel motor's stator and rotor coincides with the geometric center of the wheel. However, in practice, due to processing, manufacturing and assembly, there will be certain eccentricity between the rotor and the stator [7], [8], and under different road exciting, the tyre runout and uneven load will cause the bending of support shaft and bearing wear, which will inevitably lead to the uneven distribution of the motor air gap along the circumference [9], [10]. In addition, due to the high-speed rotation of the rotor, a large nonlinear force will be generated at the position of the bearing, which will cause the high-frequency vibration of the rotor. It can be seen that, the existence of these disturbances will be transmitted to the vehicle through the motor rotor, bearing and other transmission components, thus affecting the dynamic performance of the electric vehicle. Therefore, the influence of the coupling vibration of the rotor-bearing system on electric vehicles dynamic needs to be further studied. At present, the research in this field mainly

The associate editor coordinating the review of this manuscript and approving it for publication was Hamid Mohammad-Sedighi.

focuses on the influence of the motor exciting force on the electric vehicle dynamic performance, while the influence of the rotor-bearing coupling vibration on vehicles dynamic is seldom studied. In [11] and [12], the vertical dynamic characteristics of an electric vehicle driven by in-wheel motor under the exciting of the permanent magnet synchronous motor were studied. Based on the analysis of the exciting force of the switched reluctance motor, the influence of the suspension parameters on vehicles dynamic under the exciting force of the road and the motor was studied in [13]. By analyzing the exciting force of the switched reluctance motor, the influence of the unbalanced radial force on the vibration modes of the sprung mass and the unsprung mass was studied in [14]. In [15], the influences of the road exciting and the road-motor combined exciting on the vibration performance of an electric vehicle driven by switched reluctance motor were analyzed.

In this paper, taking a typical four-phase 8/6-pole switched reluctance motor driven electric vehicle without deceleration mechanism as an investigated object, a nonlinear dynamic model of electric vehicle with in-wheel motor driving system is established on the basis of considering the motor exciting force and the bearing nonlinear force. Through numerical simulation, the vertical dynamic characteristics of the electric vehicle driven by in-wheel motor under the coupling vibration effect of the rotor-bearing system are studied, so as to lay a foundation for improving, optimizing and controlling the vibration performance of electric vehicle driven by switched reluctance motor.

II. DYNAMIC MODEL OF THE IN-WHEEL MOTOR DRIVING SYSTEM

A. IN-WHEEL MOTOR DRIVING SYSTEM

Fig. 1 shows the structure and principle diagram of a typical in-wheel motor driving system in common use [11], [14]. The system is mainly composed of the motor, the hub, the rim, the tyre and so on. There is no deceleration mechanism in the driving system, and the in-wheel motor is a four-phase 8/6-pole switched reluctance motor with external rotor and internal stator.

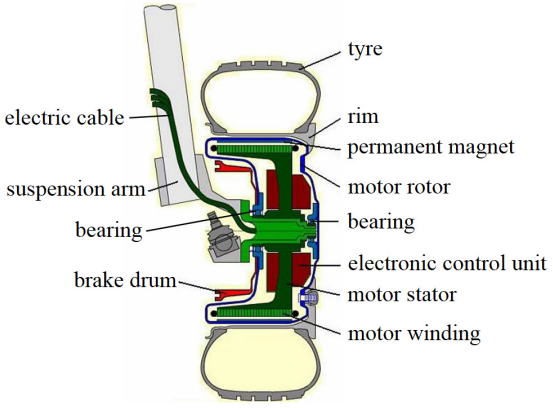

FIGURE 1. In-wheel motor driving system.

B. COUPLING DYNAMIC MODEL OF THE ROTOR-BEARING SYSTEM

According to the structure of the in-wheel motor driving system shown in Fig. 1, the coupling radial vibration model of the rotor-bearing system based on the Cartesian coordinate system is established, as shown in Fig. 2. When modeling, the following assumptions are made: (1) the system mainly includes the rotor, the left bearing, and the right bearing. Each of the three mass units is considered as a rigid body and has a translational degree of freedom in the vertical direction Z and lateral direction X; (2) the motor rotor is elastically supported on the stator by two bearings; (3) the rolling body, the inner ring, and the outer ring of the bearing are regarded as a spring-damper parallel connection system.

In Fig. 2, m_s is the total mass of the tyre, the rim and the motor rotor; m_{1l} and m_{1r} are the equivalent mass of the bearing and the stator at both ends of the bearing; C_{lx}, C_{lz}, C_{rx}, and C_{rz} are the contact damping between the inner and outer rings of the bearing and the rolling body at both ends; K_{lx}, K_{lz}, K_{rx}, and K_{rz} are the contact stiffness between the inner and outer rings of the bearing and the rolling body at both ends; e is the eccentricity of the rotor, O_1 is the geometric center of the rotor, O_2 is the centroid of the rotor.

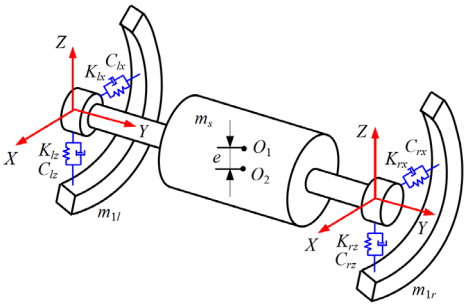

FIGURE 2. Coupling vibration model of the rotor-bearing system.

According to Newton's second law, the vibration differential equations of the system shown in Fig. 2 can be obtained by

$$\begin{cases} m_{1l}\ddot{x}_{1l} + C_{lx}(\dot{x}_{1l} - \dot{x}_s) + K_{lx}(x_{1l} - x_s) + F_{1lx} = 0 \\ m_{1l}\ddot{z}_{1l} + C_{lz}(\dot{z}_{1l} - \dot{z}_s) + K_{lz}(z_{1l} - z_s) + F_{1lz} + m_{1l}g = 0 \\ m_{1r}\ddot{x}_{1r} + C_{rx}(\dot{x}_{1r} - \dot{x}_s) + K_{rx}(x_{1r} - x_s) + F_{1rx} = 0 \\ m_{1r}\ddot{z}_{1r} + C_{rz}(\dot{z}_{1r} - \dot{z}_s) + K_{rz}(z_{1r} - z_s) + F_{1rz} + m_{1r}g = 0 \\ m_s\ddot{x}_s + C_{lx}(\dot{x}_s - \dot{x}_{1l}) + C_{rx}(\dot{x}_s - \dot{x}_{1r}) + K_{lx}(x_s - x_{1l}) \\ \quad + K_{rx}(x_s - x_{1r}) = F_{sx} + m_s e\omega_R^2 \sin\omega_R t \\ m_s\ddot{z}_s + C_{lz}(\dot{z}_s - \dot{z}_{1l}) + C_{rz}(\dot{z}_s - \dot{z}_{1r}) + K_{lz}(z_s - z_{1l}) \\ \quad + K_{rz}(z_s - z_{1r}) = F_{sz} + m_s e\omega_R^2 \cos\omega_R t - m_s g \end{cases} \tag{1}$$

where, F_{1lx}, F_{1lz}, F_{1rx}, and F_{1rz} are the nonlinear forces of the bearing in X direction and Z direction; F_{sx} and F_{sz} are the exciting forces of the motor rotor in X direction and Z direction; ω_R is the angular velocity of the rotor; x_{1l} and z_{1l} are the displacements of the left bearing in X direction and

Z direction; x_{1r} and z_{1r} are the displacements of the right bearing in X direction and Z direction; x_s and z_s are the displacements of the rotor in X direction and Z direction.

C. NONLINEAR MECHANICAL MODEL OF THE BEARING

The bearing type used in the research of the in-wheel motor driving system in this paper is a typical rolling bearing. The bearing consists of the inner ring, the outer ring, the rolling body, and the cage, in which, the inner ring of the bearing is fixed on the motor stator, and the outer ring is fixed on the motor rotor. In the study, it is assumed that there is pure rolling between the rolling body and the raceway, and the balls are arranged equidistantly between the inner and the outer raceway, in addition, the influence of the lubricating oil film is neglected. The schematic diagram of the rolling bearing model is shown in Fig. 3. In the figure, R is the radius of the outer raceway, r is the radius of the inner raceway, N_b is the number of balls, t is the time variable, and ω_R is the angular velocity of the rotor, whose value is equal to the angular velocity of the outer ring of the bearing.

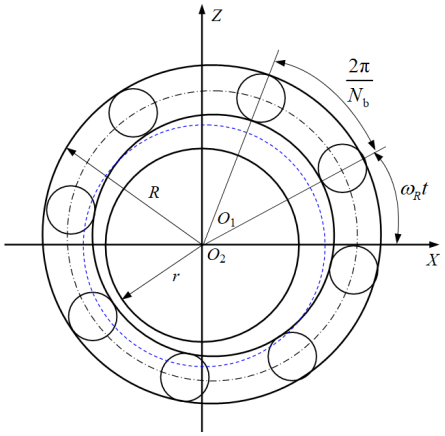

FIGURE 3. Rolling bearing model.

In the process of rolling bearing rotation, due to the existence of the nonlinear contact and the radial clearance of the bearing, the rolling bearing will show complex nonlinear dynamic characteristics, that is, the nonlinear forces of the bearing [16]. The following is an introduction to the solving process of the nonlinear forces of the bearing.

If the linear velocity of the contact point between a rolling element and the outer ring is v_o, the linear velocity of the contact point with the inner ring is v_i, the rotation angular velocity of the bearing outer ring is ω_o, and the rotation angular velocity of the bearing inner ring is ω_i, the following relations can be obtained.

$$\begin{cases} v_o = \omega_o R \\ v_i = \omega_i r \end{cases} \tag{2}$$

The linear velocity of the bearing cage (i.e., the center of the rolling body) is

$$v_c = \frac{v_o + v_i}{2} \tag{3}$$

Since the inner ring is fixed, that is, $v_i = 0$, therefore

$$v_c = \frac{v_o}{2} = \frac{\omega_o R}{2} \tag{4}$$

At this point, the angular velocity of the cage is

$$\omega_c = \frac{v_c}{(R+r)/2} = \frac{\omega_o R}{R+r} \tag{5}$$

Because the outer ring is fixed on the rotor, so the rotation angular velocity of the outer ring ω_o is equal to that of the rotor ω_R. At this point, it is known that the passing frequency of the rolling element (i.e., the variable stiffness frequency of the bearing) is as follows

$$\omega_{vc} = \omega_c N_b = \omega_o \left(\frac{R}{R+r} \cdot N_b \right) = \omega_R \left(\frac{R}{R+r} \cdot N_b \right) \tag{6}$$

If the angular position of the jth rolling element is θ_j, then the following relation can be obtained.

$$\theta_j = \omega_c t + \frac{2\pi}{N_b}(j-1), \quad j = 1, 2, \cdots, N_b \tag{7}$$

Assuming that the vibration displacements of the outer ring center in the X direction and Z direction are x and z, respectively, and assuming the bearing clearance is δ_0, then the normal contact deformation between the jth rolling body and the raceway can be obtained, that is

$$\delta_j = x \cos\theta_j + z \sin\theta_j - \delta_0 \tag{8}$$

Since only the normal positive pressure can be generated between the rolling body and the raceway, that is, only when $\delta_j > 0$ can the force be exerted between the rolling element and the raceway. Therefore, the contact pressure between the jth rolling body and the raceway can be obtained according to the nonlinear Hertzian contact theory [17].

$$F_j = K_b (x \cos\theta_j + z \sin\theta_j - \delta_0)^{\frac{3}{2}} H(x \cos\theta_j + z \sin\theta_j - \delta_0) \tag{9}$$

Here, K_b is the Hertzian contact stiffness, which is related to the material and shape of the contact body, and H is the heaviside function.

Therefore, the nonlinear forces of the bearing in the X direction and Z direction as shown in Fig. 3 can be obtained according to Equation (9), as follows

$$\begin{cases} F_x = \sum_{j=1}^{N_b} F_j \cos\theta_j \\ F_z = \sum_{j=1}^{N_b} F_j \sin\theta_j \end{cases} \tag{10}$$

D. MOTOR EXCITING FORCE MODEL

The switched reluctance motor is usually composed of the rotor, the stator, the winding, and the switching circuit. Fig. 4 shows a basic structure of a typical four-phase 8/6-pole switched reluctance motor, in which only one of the four groups of the switching circuit is drawn. Among them, there are eight salient poles in the outer circumference of the stator,

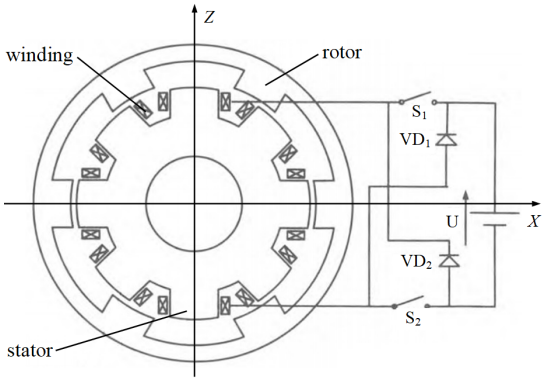

FIGURE 4. Four-phase 8/6-pole switched reluctance motor.

each salient pole is equipped with winding to form a single-pole winding, two single-pole winding opposite to the outer circumference of the stator are connected in series to form a single-phase winding. There are six salient poles in the inner circumference of the rotor, and each salient pole is called a single-phase rotor. When the single-phase rotor is close to the single-phase winding at a certain angle, the current passes through the winding coil, the flux closes along the path of the minimum reluctance, and the electromagnetic interaction between the rotor and the stator is called the single-phase rotor single-phase process. The process of the electromagnetic interaction between the single-phase rotor and all single-phase windings is called the multi-phase process of single-phase rotor; the process of the electromagnetic interaction between all single-phase rotors and all single-phase windings is called the multi-phase process of multi-phase rotor, which is the complete process of the motor exciting.

Under the linear assumption, the tangential force $F_n(t)$ and the radial force $F_r(t)$ of the single-phase process of the motor rotor can be expressed as [18]

$$F_n(t) = \begin{cases} \dfrac{Ki_A^2}{2R_m}, & (0 < t \le T_1) \\ 0, & (T_1 < t \le T_R) \end{cases} \tag{11}$$

$$F_r(t) = \begin{cases} \dfrac{i_A^2(L_{min} + K\omega_R t)}{2\sqrt{b^2 + [r_m\omega_R(T_1 - t)]^2}}, & (0 < t \le T_1) \\ 0, & (T_1 < t \le T_R) \end{cases} \tag{12}$$

where, R_m is the inner radius of the rotor, r_m is the outer radius of the stator, b is the minimum air gap between the rotor and the stator, K is the rising slope of the inductance, L_{min} is the minimum inductance, i_A is the rated current, t is the time variable, and ω_R is the angular velocity of the rotor. $T_1 = \gamma_1/\omega_R$, $T_R = 2\pi/(\omega_R N_s)$, γ_1 is the complete overlap position between the rotor and the stator, N_s is the winding series.

According to Equation (11) and Equation (12), the tangential and radial forces of the multi-phase process of single-phase rotor can be obtained as follows

$$F_n(t) = \begin{cases} \dfrac{Ki_A^2}{2R_m}, & (nT_R < t \le nT_R + T_1) \\ 0, & (nT_R + T_1 < t \le (n+1)T_R) \end{cases} \tag{13}$$

$$F_r(t) = \begin{cases} \dfrac{i_A^2[L_{min} + K\omega_R(t - nT_R)]}{2\sqrt{b^2 + (r_m\omega_R)^2[T_1 - (t - nT_R)]^2}}, \\ \qquad (nT_R < t \le nT_R + T_1) \\ 0, \quad (nT_R + T_1 < t \le (n+1)T_R) \end{cases} \tag{14}$$

In the normal operation of electric vehicles, the direction of the tangential force and the radial force of the motor changes with the change of the rotor angular displacement. Therefore, according to Equation (13) and Equation (14), the exciting force of the motor in X direction and Z direction can be obtained respectively in the multi-phase process of single-phase rotor by using the principle of force synthesis and decomposition.

$$F_{sxi}(t) = \begin{cases} \dfrac{-i_A^2[L_{min} + K\omega_R(t - nT_R)]}{2\sqrt{b^2 + (r_m\omega_R)^2[T_1 - (t - nT_R)]^2}} \sin(\omega_R t + \varphi_i) \\ + \dfrac{Ki_A^2}{2R_m}\cos(\omega_R t + \varphi_i), \quad (nT_R < t \le nT_R + T_1) \\ 0, \quad (nT_R + T_1 < t \le (n+1)T_R) \end{cases} \tag{15}$$

$$F_{szi}(t) = \begin{cases} \dfrac{-i_A^2[L_{min} + K\omega_R(t - nT_R)]}{2\sqrt{b^2 + (r_m\omega_R)^2[T_1 - (t - nT_R)]^2}} \cos(\omega_R t + \varphi_i) \\ + \dfrac{Ki_A^2}{2R_m}\sin(\omega_R t + \varphi_i), \quad (nT_R < t \le nT_R + T_1) \\ 0, \quad (nT_R + T_1 < t \le (n+1)T_R) \end{cases} \tag{16}$$

where, φ_i is the initial phase angle of the rotor at all levels.

Since the exciting force of the motor is a process of electromagnetic interaction between the single-phase rotor and all single-phase windings, the exciting force of the four-phase 8/6-pole switched reluctance motor in the X and Z directions can be obtained according to Equation (15) and Equation (16), that is

$$\begin{cases} F_{sx} = \sum_{i=1}^{N_r} F_{sxi} \\ F_{sz} = \sum_{i=1}^{N_r} F_{szi} \end{cases} \tag{17}$$

where, N_r is the number of the rotor phase.

It should be noted that, under ideal conditions, the center of the stator coincides with the rotor, that is, the minimum air gap between the rotor and the stator is a fixed value, and $b = R_m - r_m$. However, in practice, due to processing, manufacturing, and assembly, there will be certain degree of eccentricity between the rotor and the stator. Considering that

the radial force of the motor is larger and the radial unbalance force caused by the vertical eccentricity is larger, therefore, in order to facilitate the research, the minimum air gap can be obtained when the eccentricity of the rotor is vertical and the eccentricity value is e, as follows

$$b = R_{\mathrm{m}} - r_{\mathrm{m}} - e\sin\phi_k \tag{18}$$

where, ϕ_k is the initial phase angle of each stator winding.

III. DYNAMIC MODEL OF ELECTRIC VEHICLE DRIVEN BY IN-WHEEL MOTOR

In order to investigate the influence of the rotor-bearing coupling vibration on the dynamic behavior of electric vehicles driven by in-wheel motor, based on the commonly used 1/4 vehicle dynamic model (see Fig. 5(a)), a nonlinear dynamic model of electric vehicle with in-wheel motor driving system is established, as shown in Fig. 5(b). Here, MEF is the abbreviation of the motor exciting force, BNF is the abbreviation of the bearing nonlinear force.

According to Equation (1), by using Newton's second law, the vibration differential equations of the system shown in Fig. 5(b) can be obtained, as follows

$$\begin{cases} m_2\ddot{z}_2 + K_2(z_2 - z_1) + C_2(\dot{z}_2 - \dot{z}_1) + m_2 g = 0 \\ m_1\ddot{x}_1 + K_{1x}(x_1 - x_s) + C_{1x}(\dot{x}_1 - \dot{x}_s) + F_{1x} = 0 \\ m_1\ddot{z}_1 + K_{1z}(z_1 - z_s) + C_{1z}(\dot{z}_1 - \dot{z}_s) + K_2(z_1 - z_2) \\ \quad + C_2(\dot{z}_1 - \dot{z}_2) + F_{1z} + m_1 g = 0 \\ m_s\ddot{x}_s + K_{1x}(x_s - x_1) + C_{1x}(\dot{z}_s - \dot{z}_1) \\ \quad - F_{sx} - m_s e\omega_R^2 \sin\omega_R t = 0 \\ m_s\ddot{z}_s + K_1(z_s - z_1) + C_1(\dot{z}_s - \dot{z}_1) + K_t(z_s - q) \\ + C_t(\dot{z}_s - \dot{q}) - F_{sz} - m_s e\omega_R^2 \cos\omega_R t + m_s g = 0 \end{cases} \tag{19}$$

Here, m_s is the total mass of the tyre, the rim and the motor rotor; m_1 is the total mass of the bearing and the motor stator at the position of the bearing ($m_1 = m_{1l} + m_{1r}$); m_2 is the sprung mass; K_2 is the suspension stiffness; K_t is the tyre stiffness; K_{1x} and K_1 are the sum of the contact stiffness between the inner and outer rings of the bearing and the rolling body at both ends ($K_{1x} = K_{lx} + K_{rx}$, $K_1 = K_{lz} + K_{rz}$); C_2 is the suspension damping; C_t is the tyre damping; C_{1x} and C_1 are the sum of the contact damping between the inner and outer rings of the bearing and the rolling body at both ends ($C_{1x} = C_{lx} + C_{rx}$, $C_1 = C_{lz} + C_{rz}$); F_{sx} and F_{sz} are the motor exciting forces; F_{1x} and F_{1z} are the sum of the bearing nonlinear forces at both ends in X and Z directions ($F_{1x} = F_{1lx} + F_{1rx}$, $F_{1z} = F_{1lz} + F_{1rz}$; $F_{1lx} = F_{1rx} = F_x$, $F_{1lz} = F_{1rz} = F_z$); x_1 and x_s are the lateral displacements of the motor stator and the wheel (i.e., the motor rotor), respectively; z_1, z_2, and z_s are the vertical displacements of the motor stator, the car body and the wheel (i.e., the motor rotor), respectively; q is the displacement of the road roughness, in which the filter white noise model [19] is used as the input model of the road roughness in this paper, i.e., $\dot{q}(t) = -2\pi v n_{00} q(t) + 2\pi n_0\sqrt{v G_q(n_0)}w(t)$, n_0 is the reference space frequency, $n_0 = 0.1\ \mathrm{m}^{-1}$; $G_q(n_0)$ is the road power spectral density under the reference space frequency n_0; $w(t)$ is the unit white noise time domain signal; v is the vehicle running speed; n_{00} is the space cut-off frequency, $n_{00} = 0.011\ \mathrm{m}^{-1}$.

IV. VERTICAL DYNAMIC CHARACTERISTIC ANALYSIS OF ELECTRIC VEHICLE DRIVEN BY IN-WHEEL MOTOR

In order to study the influence of the coupling vibration of the rotor-bearing system on the dynamic behavior of electric vehicle driven by in-wheel motor, based on the theoretical analysis mentioned above, a numerical solution method for the nonlinear dynamic response of the electric vehicle is established by using Newmark-β numerical integration method according to Equations (10), (17), and (19), in which the stability of the solution method is ensured by adjusting the Newmark integral control parameters β and γ, and in solving the problem, let $\beta = 0.5$, $\gamma = 0.25$. An electric vehicle driven by four-phase 8/6-pole switched reluctance motor is taken as the research object, firstly, the motor exciting force and the bearing nonlinear force of the driving system are simulated, then, the dynamic performances of the electric vehicle with and without considering the motor exciting force and the bearing nonlinear force are simulated, and the dynamic performances of the electric vehicle with different suspension parameters are analyzed. Among them, the simulation conditions are B grade road surface, vehicle running speed is 50 km/h, the vehicle parameters are listed in Table 1, the in-wheel motor parameters are listed in Table 2, and the rolling bearing parameters are listed in Table 3.

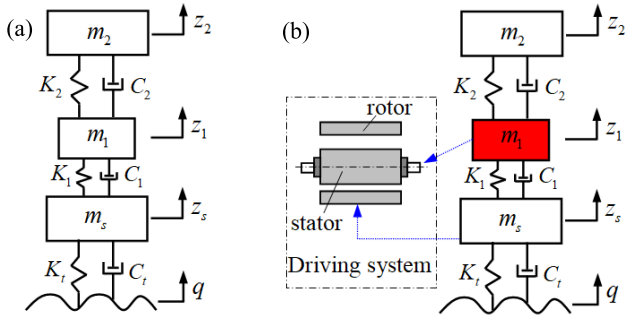

FIGURE 5. 1/4 vehicle dynamic model. (a) Traditional model (without MEF and BNF); (b) Coupling model (with MEF and BNF).

TABLE 1. Vehicle parameters.

Symbol	Unit	Value
m_2	kg	420
m_1	kg	20
m_s	kg	60
K_2	N/m	80 000
K_t	N/m	400 000
C_2	N·s/m	5 000
C_t	N·s/m	100

TABLE 2. In-wheel motor parameters.

Symbol	Unit	Value
R_m	m	0.245
r_m	m	0.244
K	-	82.5
L_{min}	H	7.24
N_r	-	6
N_s	-	8
i_A	A	7
e	m	1.5×10^{-3}
γ_1	°	21

TABLE 3. Rolling bearing parameters.

Symbol	Unit	Value
N_b	-	8
K_b	N/m	13.34×10^{9}
δ_0	m	5×10^{-6}
R	m	0.025
r	m	0.046
C_{lx}, C_{lz}, C_{rx}, C_{rz}	N·s/m	300
K_{lx}, K_{lz}, K_{rx}, K_{rz}	N/m	7.85×10^{9}
N_b	-	8

A. MOTOR EXCITING FORCE AND BEARING NONLINEAR FORCE

Fig. 6 shows the time-varying curves of the vertical exciting force of the motor under eccentricity $e = 0$ and eccentricity $e = 1.5$ mm.

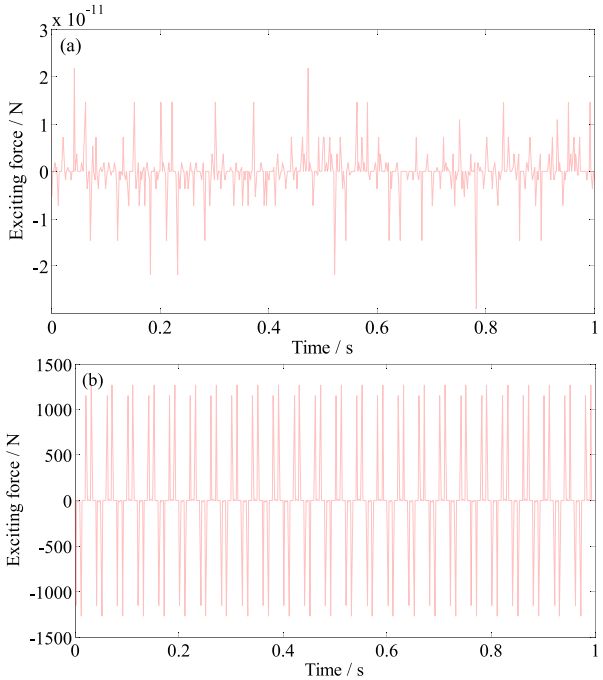

FIGURE 6. Motor exciting force. (a) $e = 0$; (b) $e = 1.5$ mm.

From Fig. 6, it can be seen that, the vertical exciting force of the motor is almost equal to zero in the ideal case (i.e., $e = 0$), and the vertical exciting force of the motor changes periodically in the case of eccentricity $e = 1.5$ mm. Thus, it can be known that, the motor does not produce vertical exciting in the ideal case of no eccentricity. However, in practice, due to processing, manufacturing, and assembly, there will be certain eccentricity between the rotor and the stator. Therefore, when analyzing the dynamic performance of electric vehicle driven by in-wheel motor, the influence of the motor exciting force should be considered comprehensively.

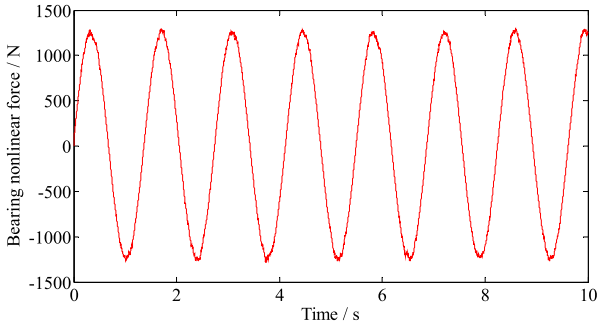

FIGURE 7. Bearing nonlinear force.

Fig. 7 shows the time-varying curve of the vertical nonlinear force of the bearing obtained by simulation. It can be seen that, the nonlinear force of the bearing varies periodically with time.

B. VERIFICATION OF THE DYNAMIC MODEL FOR ELECTRIC VEHICLE DRIVEN BY IN-WHEEL MOTOR

In order to verify the validity of the electric vehicle dynamic model established in section III (see Fig. 5(b)), a real vehicle dynamic test was carried out, as shown in Fig. 8. The comparison results of the car body vertical acceleration and the motor stator acceleration obtained by simulation and real vehicle test are shown in Fig. 9. Here, the car body vertical acceleration sensor is mounted at the position of the driver seat floor (see Fig. 8(b)), the motor stator acceleration sensor is mounted at the position of the suspension arm. The sampling frequency is 500 Hz. The sample time is 100 s, the vehicle is in full load state, the road grade is B, and the vehicle test speed is 50 km/h. The parameters of the test vehicle are shown in Table 1.

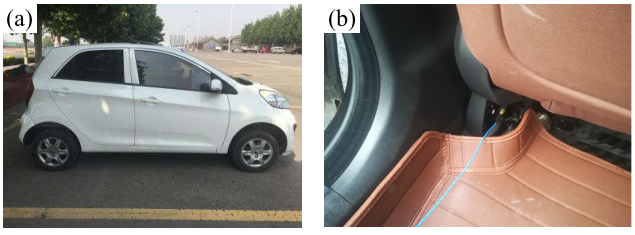

FIGURE 8. Onsite test of vehicle dynamics. (a) Test vehicle; (b) Sensor arrangement of the car body vertical acceleration.

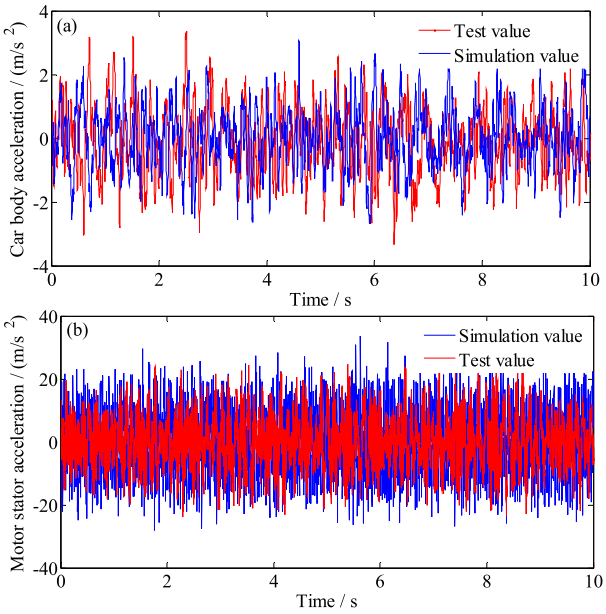

FIGURE 9. Comparison results of the car body vertical acceleration and the motor stator acceleration obtained by simulation and real vehicle test. (a) Car body vertical acceleration; (b) Motor stator acceleration.

As can be seen from Fig. 9, the simulation results of the car body vertical acceleration and the motor stator acceleration are in good agreement with the test results, in which, the root mean square values of the car body vertical acceleration and the motor stator acceleration obtained by simulation are 0.79 m/s^2, 8.61 m/s^2, the test values are 0.83 m/s^2, 8.25 m/s^2. The results show that the dynamic model established is correct.

C. INFLUENCE OF THE ROTOR-BEARING COUPLING VIBRATION ON THE ELECTRIC VEHICLE DYNAMIC BEHAVIOR

With considering and unconsidering the motor exciting force (MEF) and the bearing nonlinear force (BNF), the simulation results of the dynamic performance of the electric vehicle driven by in-wheel motor are obtained, as shown in Fig. 10 and Table 4.

From Fig. 10 and Table 4, it can be seen that, the influence of the rotor-bearing coupling vibration on the dynamic behavior of the electric vehicle is mainly embodied in the tyre vibration acceleration and the tyre dynamic load. The introduction of the motor exciting force of the switched reluctance motor and the nonlinear force of the supporting bearing makes the tyre vibration acceleration and the tyre dynamic load deteriorate sharply. In addition, when considering the rotor-bearing coupling vibration, the suspension dynamic deflection is almost unchanged, but the car body vibration acceleration increases. It can be known that, the existence of the rotor-bearing coupling vibration reduces the ride comfort and driving safety of electric vehicles.

In order to further show the relative effect of eccentricity and relevance of additional forces in comparison to ideal conditions, Table 5 gives the simulation results of the dynamic performance of the electric vehicle driven by in-wheel motor with considering and unconsidering the road exciting.

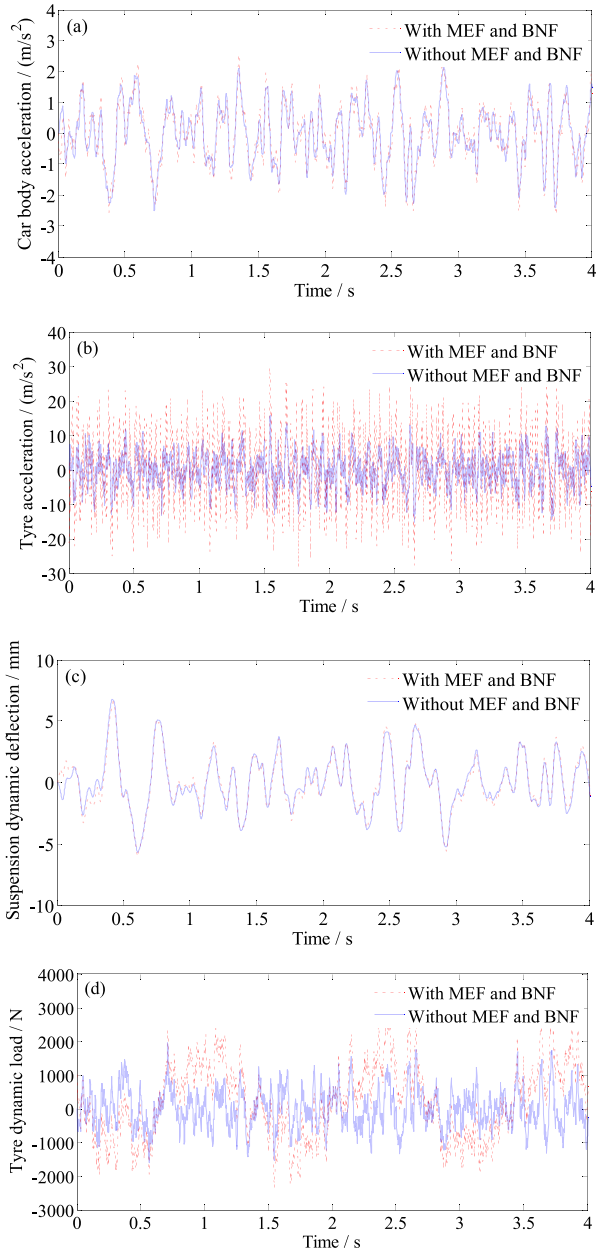

FIGURE 10. Simulation results of the vertical vibration characteristics of electric vehicle driven by in-wheel motor. (a) Car body acceleration; (b) Tyre acceleration; (c) Suspension dynamic deflection; (d) Tyre dynamic load.

TABLE 4. Root mean square (RMS) values of each vibration response.

RMS	With MEF and BNF	Without MEF and BNF
Car body acceleration/(m/s^2)	0.79	0.75
Tyre acceleration/(m/s^2)	8.61	5.07
Suspension dynamic deflection/(mm)	2.44	2.43
Tyre dynamic load/(N)	1 101.37	594.10

TABLE 5. Root mean square (RMS) values of each vibration response.

RMS	With road exciting	Without road exciting
Car body acceleration/(m/s^2)	0.79	0.10
Tyre acceleration/(m/s^2)	8.61	6.93
Suspension dynamic deflection/(mm)	2.44	0.34
Tyre dynamic load/(N)	1 101.37	912.75

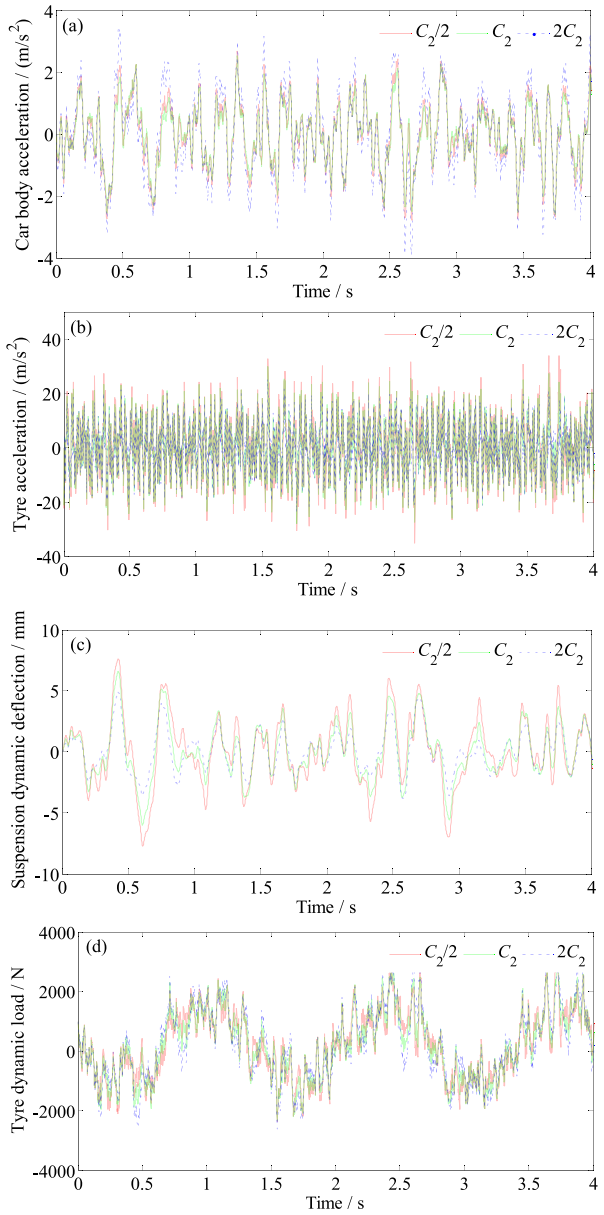

FIGURE 11. Influence of the suspension damping on the dynamic behavior of electric vehicle driven by in-wheel motor. (a) Car body acceleration; (b) Tyre acceleration; (c) Suspension dynamic deflection; (d) Tyre dynamic load.

As can be seen from Table 5, considering the road exciting or not, there are great differences in the car body vibration acceleration and the suspension dynamic deflection between the two excitation models, that is to say, the rotor-bearing coupling vibration on the dynamic behavior of the electric vehicle is mainly embodied in the tyre vibration acceleration and the tyre dynamic load.

D. DYNAMIC ANALYSIS OF ELECTRIC VEHICLE WITH DIFFERENT SUSPENSION PARAMETERS

Fig. 11 shows the dynamic behavior of the electric vehicle driven by in-wheel motor when only the suspension damping parameter changes while other parameters remain unchanged. Table 6 gives the root mean square calculation results of each vibration response.

TABLE 6. Root mean square (RMS) values of each vibration response.

RMS	$C_2/2$	C_2	$2C_2$
Car body acceleration/(m/s^2)	0.85	0.79	1.11
Tyre acceleration/(m/s^2)	9.89	8.61	7.58
Suspension dynamic deflection/(mm)	3.27	2.44	1.77
Tyre dynamic load/(N)	1 116.97	1 101.37	1 152.93

It can be seen From Fig. 11 and Table 6, the car body acceleration decreases first and then increases with the increase of C_2, while the tyre acceleration and the suspension dynamic deflection decrease with the increase of C_2. The change trend of the tyre acceleration and the suspension dynamic deflection is basically the same. In addition, the tyre dynamic load first decreases and then increases with the increase of C_2, but the change range is small. Thus, from the requirements of the tyre acceleration and the suspension dynamic deflection, the greater of the suspension damping, the better, and for the car body acceleration, there is an optimal damping to make the vehicle evaluation index achieve the best performance.

Fig. 12 shows the dynamic behavior of the electric vehicle driven by in-wheel motor when only the suspension stiffness parameter changes while other parameters remain unchanged. Table 7 gives the root mean square calculation results of each vibration response.

As can be seen from Fig. 12 and Table 7, the car body acceleration increases with the increase of K_2, the less the suspension stiffness, the less the car body acceleration, and the other vibration responses change little with the increase of K_2.

As stated above, the existence of the in-wheel motor driving system will deteriorate the evaluation index of the electric vehicle vibration performance. By choosing appropriate parameters of the vehicle suspension system, the ride comfort of the electric vehicle can be effectively improved. Therefore, compared with the traditional research methods (neglecting the rotor-bearing coupling vibration), the introduction of the switched reluctance motor driving system makes the vibration performance of electric vehicles face many new problems. It is necessary to conduct a more comprehensive study and analysis on the vibration performance of electric vehicles

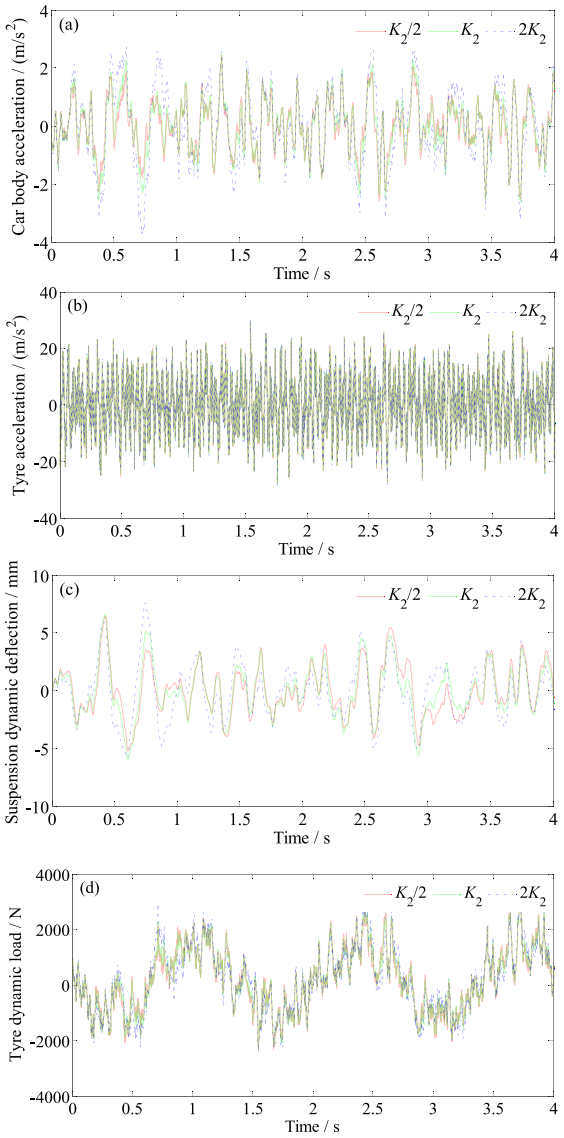

FIGURE 12. Influence of the suspension stiffness on the dynamic behavior of electric vehicle driven by in-wheel motor. (a) Car body acceleration; (b) Tyre acceleration; (c) Suspension dynamic deflection; (d) Tyre dynamic load.

driven by switched reluctance motor and even all in-wheel motors, so as to lay a solid foundation for improving, optimizing, and controlling the vibration performance of electric vehicles.

TABLE 7. Root mean square (RMS) values of each vibration response.

RMS	$K_2/2$	K_2	$2K_2$
Car body acceleration/(m/s^2)	0.70	0.79	1.08
Tyre acceleration/(m/s^2)	8.61	8.61	8.63
Suspension dynamic deflection/(mm)	2.46	2.44	2.43
Tyre dynamic load/(N)	1 097.36	1 101.37	1 147.75

V. CONCLUSION

In this paper, taking a typical four-phase 8/6-pole switched reluctance motor driven electric vehicle without deceleration mechanism as an investigated object, a nonlinear dynamic model of electric vehicle with in-wheel motor driving system is established on the basis of considering the motor exciting force and the bearing nonlinear force. Through numerical simulation, the vertical dynamic characteristics of electric vehicle driven by in-wheel motor under the coupling vibration effect of the rotor-bearing system are studied. The results show that, the influence of the rotor-bearing coupling vibration on the dynamic behavior of the electric vehicle is mainly embodied in the tyre vibration acceleration and the tyre dynamic load. The introduction of the switched reluctance motor exciting force and its support bearing nonlinear force makes the tyre vibration acceleration and the tyre dynamic load deteriorate sharply. After considering the rotor-bearing coupling vibration, the suspension dynamic deflection is almost unchanged, and the car body vibration acceleration is increased. The existence of the rotor-bearing coupling vibration reduces the ride comfort and driving safety of electric vehicles. By choosing appropriate suspension system parameters, this problem can be effectively reduced. This study can provide an effective model reference for the research of vibration performance of the switched reluctance motor driven electric vehicle and the improvement, optimization, and control of its vibration performance.

REFERENCES

[1] E. Katsuyama, "Decoupled 3D moment control using in-wheel motors," *Vehicle Syst. Dyn.*, vol. 51, no. 1, pp. 18–31, 2013.

[2] Y. Hori, "Future vehicle driven by electricity and control-research on four-wheel-motored 'UOT electric march II,'" *IEEE Trans. Ind. Electron.*, vol. 51, no. 5, pp. 954–962, Oct. 2004.

[3] X. Shao, F. Naghdy, H. Du, and Y. Qin, "Coupling effect between road excitation and an in-wheel switched reluctance motor on vehicle ride comfort and active suspension control," *J. Sound Vibrat.*, vol. 443, pp. 683–702, Mar. 2019.

[4] W. Tong and Z. Hou, "Vertical vibration analysis on electric vehicle with suspended in-wheel motor drives," in *Proc. World Electr. Vehicle Symp. Exhib.*, Barcelona, Spain, Nov. 2014, pp. 1–9.

[5] D. Tan and Q. Wang, "Modeling and simulation of the vibration characteristics of the in-wheel motor driving vehicle based on bond graph," *Shock Vibrat.*, vol. 2016, Oct. 2016, Art. no. 1982390.

[6] M. Liu, F. Gu, J. Huang, C. Wang, and C. Cao, "Integration design and optimization control of a dynamic vibration absorber for electric wheels with in-wheel motor," *Energies*, vol. 10, no. 12, p. 2069, 2017.

[7] J. Li, X. Gao, P. Wang, and Z. Zhang, "Vibration analysis of e1ectric vehicle under the action of road and switched reluctance motor," *J. Hunan Univ. (Natural Sci.)*, vol. 45, no. 8, pp. 7–14, 2018.

[8] J. Wang, Z. P. Xia, S. A. Long, and D. Howe, "Radial force density and vibration characteristics of modular permanent magnet brushless AC machine," *IEE Proc.-Electr. Power Appl.*, vol. 153, no. 6, pp. 793–801, Nov. 2006.

[9] J. Li and Y. Cho, "Dynamic reduction of unbalanced magnetic force and vibration in switched reluctance motor by the parallel paths in windings," *Math. Comput. Simul.*, vol. 81, pp. 407–419, Oct. 2010.

[10] J. T. Li, Z. J. Liu, and L. H. A. Nay, "Effect of radial magnetic forces in permanent magnet motors with rotor eccentricity," *IEEE Trans. Magn.*, vol. 43, no. 6, pp. 2525–2527, Jun. 2007.

[11] Y. Luo and D. Tan, "Study on the dynamics of the in-wheel motor system," *IEEE Trans. Veh. Technol.*, vol. 61, no. 8, pp. 3510–3518, Oct. 2012.

[12] D. Tan and C. Lu, "The Influence of the magnetic force generated by the in-wheel motor on the vertical and lateral coupling dynamics of electric vehicles," *IEEE Trans. Veh. Technol.*, vol. 65, no. 6, pp. 4655–4688, Jun. 2016.
[13] Y. Qin, C. He, X. Shao, H. Du, C. Xiang, and M. Dong, "Vibration mitigation for in-wheel switched reluctance motor driven electric vehicle with dynamic vibration absorbing structures," *J. Sound Vibrat.*, vol. 419, pp. 249–267, Apr. 2018.
[14] Z. Li, L. Zheng, Y. Ren, Y. Li, and Z. Xiong, "Multi-objective optimization of active suspension system in electric vehicle with in-wheel-motor against the negative electromechanical coupling effects," *Mech. Syst. Signal Process.*, vol. 116, pp. 545–565, Feb. 2019.
[15] J. Li, X. Gao, and P. Wang, "An analysis on the influence of switched reluctance motor and road on the vibration of electric vehicle," *Automot. Eng.*, vol. 40, no. 4, pp. 411–416, 2018.
[16] Y. Chi, S. Yang, W. Jiao, J. He, X. Gu, and E. Papatheou, "Spectral DCS-based feature extraction method for rolling element bearing pseudo-fault in rotor-bearing system," *Measurement*, vol. 132, pp. 22–34, Jan. 2019.
[17] G. Chen, "Rotor-ball bearing-stator coupling dynamic model including rubbing coupling faults," *J. Vibrat. Eng.*, vol. 20, no. 4, pp. 361–368, 2007.
[18] Y. C. Xue, Y. M. Zhang, and X. D. He, "Research on exciting of SR motor on electric vehicle," *J. Agricult. Machinery*, vol. 39, no. 2, pp. 25–29, 2008.
[19] Y. Li, W. Sun, J. Huang, L. Zheng, and Y. Wang, "Effect of vertical and lateral coupling between tyre and road on vehicle rollover," *Vehicle Syst. Dyn.*, vol. 51, no. 8, pp. 1216–1241, 2013.

YUEWEI YU was born in Shandong, China, in 1989. He received the B.Sc. and M.Sc. degrees from the Shandong University of Technology, Zibo, China, in 2013 and 2017, respectively, where he is currently pursuing the Ph.D. degree in mechanical engineering.

His research interests include vehicle dynamics, system modeling and simulation, and control strategy of vehicles.

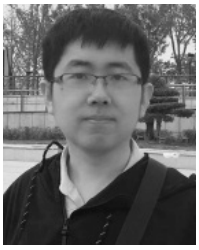

LEILEI ZHAO was born in Shandong, China, in 1982. He received the B.Sc. degree from Shandong Jianzhu University, in 2008, and the M.Sc. degree from the Shandong University of Technology, in 2011. He is currently pursuing the Ph.D. degree in mechanical and electronic engineering with the Beijing University of Posts and Telecommunications.

His research interests include vehicle dynamics and system modeling.

CHANGCHENG ZHOU was born in Shandong, China, in 1962. He received the B.Sc. degree from the Shandong University of Technology, in 1986, the M.Sc. degree from Jiangsu University, in 1993, and the Ph.D. degree from the Beijing Institute of Technology, in 2006. Since 2004, he has been a Professor with the Shandong University of Technology, Zibo, China.

His research interests include vehicle dynamics and control strategy of vehicles.